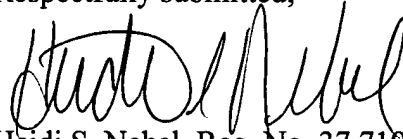


REMARKS

Applicant has inserted Sequence ID numbers into the specification to more clearly identify the alpha and beta subunits of insulin described in this application.

Attached hereto is a marked-up version of the changes made to the specification by the current amendment. The attached page is captioned "**Version with markings to show changes made.**"

Respectfully submitted,



Heidi S. Nebel, Reg. No. 37,719

ZARLEY, McKEE, THOMTE, VOORHEES
& SEASE

801 Grand Avenue, Suite 3200

Des Moines, Iowa 50309-2721

Phone No. (515) 288-3667

Fax No. (515) 288-1338

CUSTOMER NO: 22885

Attorneys of Record

- pw -

Application No. P04885US1



**AMENDMENT — VERSION WITH MARKINGS
TO SHOW CHANGES MADE**

In the Specification

Please change the paragraph beginning at page 2, line 3 as follows:

Diabetes is presently treated by insulin replacement therapy. This treatment has been very successful, but it still has problems such as glycemic control. Poor glycemic control can cause retinopathy, poor blood circulation and the other problems associated with diabetes. It is also difficult to formulate insulin for slow release. Modified insulins have been created in an attempt to address problems with insulin therapy. In some cases, “super-insulins” have been created to increase the activation of insulin receptor by its ligand. In other cases, binding to insulin receptor is not substantially increased, but the ligand has more favourable formulation properties. For example, in Humalog™ (SEQ ID NO:3 and SEQ ID NO:4), a lysine and a proline in insulin are switched to provide more favourable solubility characteristics.

Please change the paragraph beginning at page 3, line 27 as follows:

The details of the insulin binding site provide an explanation of binding of normal human insulin (including recombinantly produced insulin such as Novolin™) as well as of the lesser or greater binding of insulin from other animals to the human IR (SEQ ID NO:15, SEQ ID NO:16 and SEQ ID NO:17) and explains the binding of modified insulins such as “super-insulins”, Humalog™ (SEQ ID NO:3 and SEQ ID NO:4) and other insulin analogs.

Please change the paragraph beginning at page 12, line 3 as follows:

Figure 1. Receptor-binding assay of Nanogold-insulin. Receptor-binding activity of purified Nanogold-insulin was compared to that of bovine insulin (SEQ ID NO:11 and SEQ ID NO:12) in a receptor-binding assay using human insulin receptor as described (9). Inset shows the mass spectrum obtained from the MOLDI-TOF analysis of purified Nanogold-insulin (7).

Please change the paragraph beginning at page 15, line 2 as follows:

Sequential spatial arrangement of the subdomains of one $\alpha\beta$ monomer of the insulin receptor deduced from the 3D structure [1]. The N-terminal of the α subunit (SEQ ID NO:16) is at the top, the C-terminal of the β subunit (SEQ ID NO:17) near the bottom. The domains and their delimiting amino acid sequences [5] are: α N-terminal - 1 - L1 - 158/159 - cysteine-rich (CR) - 310/311 - L2 - 470/471 - connecting-domain/ α Fibronectin0 (CD/Fn0) -572/573 - α Fibronectin1 (α Fn1) - 661/662 - α -insert-domain (ID)- 719 - α C-terminal; β N-terminal - 724 - β -ID - 779/780 - β Fn1 - 816/817 - β Fn2 -913/914 - juxtamembrane - 929/930 - transmembrane (TM) - 952/953 - juxtamembrane - 977/978 - tyrosine-kinase (TK) - 1283/1284 - C-terminal region - 1388 - β C-terminal. Other important residues are Cys524 (denoted by "1"), which forms an α - α bond on the two-fold symmetry axis, as does one of Cys682, Cys683 or Cys685 (shown as "2") . An α - β bond is formed by Cys647 in Fn1 of the α subunit (SEQ ID NO:16) and Cys872 in Fn2 of the β subunit (SEQ ID NO:17) (shown as "3"). "x" marks the cleavage site between the α (SEQ ID NO:16) and β (SEQ ID NO:17) subunits in the pro-receptor. The catalytic loop and the activation loop (shown as "A-C"; residues 1130-37 and 1149-70, respectively) are approximately in the central region of the tyrosine kinase structure [10,11].

Please change the paragraph beginning at page 16, line 10 as follows:

Simplified schematic of structural changes during activation of insulin receptor. **a.** Inhibitory state. Ectodomain of dimeric α subunits (SEQ ID NO:16) each with two differing insulin binding sites and blocking cam. Unbound bivalent insulin. β subunits (SEQ ID NO:17) resting against cams, crossing membrane, with tyrosine kinase (TK) domains separated. Arrows indicate thermally induced motion. **b,** Insulin bound state. Blocking cams rotated, β subunits (SEQ ID NO:17) resting against centre of ectodomain. TK domains juxtaposed for transphosphorylation.

Please change the paragraph beginning at page 17, line 2 as follows:

Sequence of (a) human insulin (SEQ ID NO:9 and SEQ ID NO:10) (b) cow insulin (SEQ ID NO:11 and SEQ ID NO:12) (c) pig insulin (SEQ ID NO:13 and SEQ ID NO:14).

Please change the paragraph beginning at page 17, line 4 as follows:

Sequence of human insulin receptor (SEQ ID NO:15, SEQ ID NO:16 and SEQ ID NO:17).

Please change the paragraph beginning at page 19, line 26 as follows:

The determination of the quaternary structure of IR, and in particular its fitted quaternary structure, provides a basis for the design of new and specific compounds for the diagnosis and/or treatment of IR-related pathologies ("pathology" includes a disease, a disorder and/or an abnormal physical state preferably characterized by either (i) inadequate or excessive insulin in a mammal (preferably a human) or inadequate or excessive IR (SEQ ID NO:15, SEQ ID NO:16 and SEQ ID NO:17) activity. IR related pathologies include those involving IR as in fig. 12 or IR variants described in this application.). This structure is useful in the design of modulators (agonists or antagonists), which may be used as therapeutic or prophylactic compounds for treating pathologies in which upregulation or downregulation of receptor activity is beneficial. It will be apparent that methods using IR described below may be readily adapted for use with a fragment of IR or an IR variant.

Please change the paragraph beginning at page 25, line 1 as follows:

Human insulin (SEQ ID NO:1 and SEQ ID NO:2)

Please change the paragraph beginning at page 25, line 5 as follows:

Humalog (SEQ ID NO:3 and SEQ ID NO:4)

Please change the paragraph beginning at page 25, line 13 as follows:

Bovine Insulin (SEQ ID NO:5 and SEQ ID NO:6)

Please change the paragraph beginning at page 25, line 19 as follows:

Pig Insulin (SEQ ID NO:7 and SEQ ID NO:8)

Please change the paragraph beginning at page 43, line 14 as follows:

Insulin receptor protein (HIR (SEQ ID NO:15, SEQ ID NO:16 and SEQ ID NO:17)) was solubilized from human placental membranes and purified by affinity chromatography on an insulin column (9) followed by further FPLC purification on Sephacryl S-200. The purity of HIR (SEQ ID NO:15, SEQ ID NO:16 and SEQ ID NO:17) was better than 95% by sodium dodecyl sulfate polyacrylamide gel electrophoresis. HIR (SEQ ID NO:15, SEQ ID NO:16 and SEQ ID NO:17) was incubated with NG-BI (final concentration of $\sim 0.5 \times 10^{-6}$ M) at 4° C overnight in 20 mM

HEPES buffer (pH 7.5) at a molar ratio of insulin:HIR of $\sim 10:1$. Free NG-BI was removed by microfiltration with a cut-off of 300 kDa (Sigma). The mixture was diluted to 7.5 μg of receptor protein/ml with 20 mM HEPES buffer, pH 7.5, prior to loading on the grid.

Please change the paragraph beginning at page 44, line 4 as follows:

The quaternary structure of IR bound to insulin was determined by marking with Nanogold. The 70 atom gold marker localized and delimited the insulin binding site. Compared to native bovine insulin, Nanogold-bovine-insulin (NG-BI), derivatized at the B-chain Phe1^(vi), a location not directly involved in receptor binding (^{vii}), bound to human insulin receptor (HIR) (SEQ ID NO:15, SEQ ID NO:16 and SEQ ID NO:17) with only a slightly reduced affinity (Fig. 1). Purified solubilized HIR (SEQ ID NO:15, SEQ ID NO:16 and SEQ ID NO:17) used in this study has been shown to be fully active (^{viii}). Such HIR (SEQ ID NO:15, SEQ ID NO:16 and SEQ ID NO:17), incubated with NG-BI to form the HIR/NG-BI complex in the absence of ATP, was subjected to low-dose dark field STEM imaging at -150°C . Figure 2A shows a representative field of individual molecules. On average, each HIR/NG-BI complex measured 15 nm across. Based on its strong scattering, the 1.4 nm gold ligand of NG-BI was located on the image directly as a clear site of highest density, or could be demonstrated as such by thresholding. Figure 2B shows examples of molecules with 1 or 2 sites of highest density, indicative of binding of one or occasionally two NG-BI particles, consistent with the known binding of between one and two insulins per IR (3). When two NG-BI particles were detected, they were in close proximity to each other.

Please change the paragraph beginning at page 46, line 6 as follows:

In the side views, the top part of the structure, where NG is located, is identified as the ectodomain of the α subunit (SEQ ID NO:16). The dog-bone-shaped substructure of the 3D reconstruction, (Fig. 3B, top view), and equivalently the top-most, bow-tie-shaped structure (Fig. 3B, 0°), are designated as the two L1 domains of the dimeric receptor on the basis of the x-ray structure of the L1-Cys-rich-L2 domains. The side view at 65° shows the L1-Cys-rich-L2 domains as contiguous substructures across the upper central region of the molecule, with enough additional volume in this region to account for most of the remaining mass of the two α subunits, primarily the connecting domains (CD).

Please change the paragraph beginning at page 46, line 14 as follows:

The contiguity of the domain structure (Fig. 3B, top and side view 90°), along with the primary domain sequence (Fig. 4A), shows that the two β subunits (SEQ ID NO:17) occupy the lower half of the structure, distal from L1, reaching up and out as a contiguous mass. The intracellular TK domain of IR would then occupy the bottom portion of this structure with two IR

fibronectin type III (FnIII) repeats in each receptor half being in the top portion of the crescent-shaped spiral of the β subunit (SEQ ID NO:17) at the same level as the L2 domain in the α subunit (SEQ ID NO:16). One of the FnIII repeats, composed of residues from both the α (SEQ ID NO:16) and β subunit (SEQ ID NO:17), is assigned to the upper left end of the crescent (side view, 0°) where it is contiguous with the CD portion of the α subunit (SEQ ID NO:16) (top view). Fig. 4C and 4D (cf. Fig. 3B, 90°, top view, respectively) show the fitting of the crystal structure of the TK domain of the β subunit (SEQ ID NO:17) and of the two FnIII repeats modelled as the canonical fibronectin type III structures (16).

Please change the paragraph beginning at page 46, line 26 as follows:

The masses of the kinase domains are connected via a slender horizontal bridge (Fig. 3B, side view 90°) that was not observed in the x-ray structures of the TKs, but can be explained in terms of the reconstruction being in a transition between free IR and its ligand-activated form. In the two symmetrically fitted TK (Fig. 4C and 4D) crystal structures the catalytic loops are separated by 4 nm. This distance is just sufficient to permit the tyrosine triplet (Tyr1158, 1162 and 1163) in a fully extended flexible activation loop of one TK to reach the catalytic loop of the opposite TK as modelled from the x-ray coordinates (PDB 1IRp). The extension of the activation loops, equivalent in cross-section to four extended polypeptide chains, easily accounts for the linking density observed between the lower portions of the β subunits (SEQ ID NO:17) (Fig. 3B, 90°). This is an important difference from the x-ray structures of the inactive and activated TKs as discussed below.

Please change the paragraph beginning at page 47, line 7 as follows:

The spatial relationship between the domains of the α (SEQ ID NO:16) and β (SEQ ID NO:17) subunits (e.g. side view, 90°) shows the location of the cell membrane lipid bilayer as the space below the α subunits (SEQ ID NO:16) and above the bridge linking the two assigned TK domains. Instead of a flat open region, this space in the 3D reconstruction forms a thick dome-like slab above the bridge with a thickness variation of 2.2 to 2.7 nm. This spacing is a change in shape from, and a decrease in the thickness expected for a membrane bilayer that would accommodate an alpha-helical transmembrane domain (TM) of 23-26 hydrophobic amino acids. However, since the purified IR in the absence of its native membrane was fully active, the relative positions of the extracellular and intracellular domains must still represent a close to native arrangement.

Please change the paragraph beginning at page 47, line 17 as follows:

The crossing L1-Cys-rich-L2 domains of the dimeric α subunits (SEQ ID NO:16) were presented (Fig. 4B and 4C). We determined the x-ray coordinates with IR from the domain structures (5) (See Fig. 7). Using this structure, the localization of the gold cluster, and the

known receptor-binding domain of insulin (8), we have fitted an NG-BI molecule into this region. The best fit is obtained with a molecule of insulin, partially on the two-fold symmetry axis of the dimer, being in contact with the L1-Cys-rich domains of one α subunit (SEQ ID NO:16) and with the L2 domain of the other α subunit (SEQ ID NO:16). A model involving both α subunits (SEQ ID NO:16) in the high-affinity binding of insulin has previously been proposed based on studies of insulin analogues binding to IR and IR/IGF-I R chimeras (^{ix}). Our 3D reconstruction shows this involvement. Although two molecules of insulin can be fitted to this configuration, two molecules of Nanogold-labeled insulin were observed only rarely in the STEM images. The high-affinity binding of the first insulin molecule to the IR has induced a conformational change in the binding domain so that the second insulin molecule would bind only at low affinity. Likewise the binding of a second molecule of insulin could effect a conformational change that enhances the dissociation of the bound insulin. Thus the curvilinear Scatchard plot and the negative cooperativity of insulin binding (^x) can be explained on the basis of the 3D reconstruction. The reconstruction also explains why only low-affinity binding is obtained with purified $\alpha\beta$ monomer.

Please change the paragraph beginning at page 48, line 24 as follows:

The 3D structure obtained from images of the HIR complex containing only a single NG-BI, shows that one molecule of insulin is sufficient to bring the two $\alpha\beta$ monomers to an activating configuration. The dimeric receptor with a Ser323Leu mutation in the L2 domain of both α subunits (SEQ ID NO:16) showed a severe impairment in insulin binding, whereas a hybrid receptor with only one of the two α subunits (SEQ ID NO:16) mutated was found to bind insulin with high affinity and was fully active as a tyrosine kinase. Based on our 3D reconstruction, insulin bound to the L1 domain of the mutant α subunit (SEQ ID NO:16) and the wild-type L2 domain of the hybrid IR and the binding of only a single molecule of insulin is sufficient for TK activation.

Please change the paragraph beginning at page 50, line 20 as follows:

Covalent linking of the two monomers of IR occurs between Cys524 of each monomer, and also between corresponding Cys682 (or 683 or 685) moieties^{4,7}. Each monomer itself contains a 135 kDa α subunit (SEQ ID NO:16) and a 95 kDa β subunit (SEQ ID NO:17) linked by a single disulphide bond (α Cys647 to β Cys872)⁴. The structure of one monomer is diagrammed in Fig. 6. From considerations of symmetry of the $(\alpha\beta)_2$ dimer, the two α - α disulphide bonds^{5,7} occur one above the other on the two-fold symmetry axis of the dimer (labelled 1 and 2, Fig. 6). In the interpretation of the 3D structure, two polypeptide chains link the β subunit from fibronectin domain Fn1 to the connecting domain CD/Fn0 and insert domain ID of the central α subunit.

Please change the paragraph beginning at page 50, line 29 as follows:

Crystal structures were determined only for parts of IR: the intracellular TK domain in the unphosphorylated state as well as phosphorylated and bound to a peptide substrate^{8,9}, and the first three extracellular domains, L1, Cys-rich, and L2, of the homologous type 1 insulin-like growth factor receptor (IGF-1R)¹⁰. From analysis of sequence homology each $\alpha\beta$ monomer contains three fibronectin type III repeats^{11,13,31}. The ID of the α subunit (SEQ ID NO:16), the transmembrane and juxtamembrane regions and the ID and C-terminal domains of the β subunit (SEQ ID NO:17) are still of unknown structure.

Please change the paragraph beginning at page 52, line 19 as follows:

The linkage in the ectodomain between the L1-CR-L2 regions and the IR transmembrane domain is via three fibronectin type III (Fn) domains and two so-called insert domains, one each on the α (SEQ ID NO:16) and β (SEQ ID NO:17) subunits of each monomer. This region also provides the two disulphide bonds that covalently link the $\alpha\beta$ monomers to form the constitutive IR dimer. One disulphide bond occurs between the Fn0 domains of the α subunits (SEQ ID NO:16), the other between corresponding α insert domains (Fig. 6). Two of the Fn domains, Fn1 and Fn2 are not involved in dimer formation, and have been modelled into the 3D reconstruction previously as the normal seven-beta-strand fibronectin type III structure¹, even though Fn1 is made up of four beta strands from the α subunits (SEQ ID NO:16) and three from the β subunit⁶ (SEQ ID NO:17).

Please change the paragraph beginning at page 54, line 13 as follows:

The structural basis for the proposed mechanism of IR transmembrane signal transduction is depicted in Fig. 9, pared to a two-dimensional representation. In the inactive state (Fig. 9a) the β subunit (SEQ ID NO:17) transmembrane regions and the associated intracellular TKs are held apart by the cam-like blocks on the central portion of the dimeric α ectodomain. The open extracellular structure of the IR dimer shows that the two sets of L1-CR regions are splayed apart. When a single insulin molecule with its two different binding regions¹⁵ attaches to a contralateral pair of the four binding sites of the two α subunits¹⁶ (SEQ ID NO:16), the bumper-like cam regions are rotated and lifted out of the way of the extracellular domains of the β subunits (Fig. 9b). The closed structure is based on the 3D reconstruction¹.

Please change the paragraph beginning at page 54, line 23 as follows:

A more realistic depiction of the contiguous three-dimensional structural features of the IR dimer (Fig. 5a), that alternately permit and prevent TK activation, is the set of connected cylinders in Figs. 5b and 5c. The perspective of Figs. 5b(ii) and 5c(ii) is similar to Fig. 9. The insulin-binding domains, L1 and Cys-rich (CR), of each monomer (one blue, one fuchsia), cross

symmetrically near the middle of the structure. They are attached to the L2, CD/Fn0 and ID domains, modelled as contiguous central barrel structures joined together on the two-fold symmetry axis via the two inter-monomer disulphides (labelled 1,2 in Figs. 5b and 5c). The cam-like protrusions on the CR domains, represented as discs, abut the Fn2 domains of the β subunits (SEQ ID NO:17). These protrusions can just be seen in the high-density representation of the 3D reconstruction (cam, Fig. 5a). The mass of the cam reaches across from the centre to the Fn2 region in the full-volume representation (Fig. 7b). Near the CD/Fn0 ends of the barrels, each α subunit (SEQ ID NO:16) structure extends sideways to help form the Fn1 repeat and to tether each β subunit (SEQ ID NO:17) by a flexible joint to the central structure.

Please change the paragraph beginning at page 55, line 6 as follows:

The N-terminal domain of the β subunit (SEQ ID NO:17) starts near the CD/Fn0 side arm of the α subunit (SEQ ID NO:16) (Fig. 6), leading into Fn1 and Fn2 of the extracellular domain of IR (Figs. 5b and 5c). At that point the β subunit (SEQ ID NO:17) forms an axle-like transmembrane (TM) region⁴, crossing the membrane before folding into the TK domain. Flexible activation loops (A) of both TKs^{8,9} are modelled as extending towards the catalytic region of the opposite TK (Fig. 5c(iii)).

Please change the paragraph beginning at page 57, line 30 as follows:

The IR is activated artificially by removal of amino acids 1 to 578 through tryptic digestion¹⁹. This cleavage still retains covalent links between the monomers and between the alpha (SEQ ID NO:16) and beta (SEQ ID NO:17) subunits. However, the insulin-binding region and the CR domains have been removed, along with their physical "cam structures". Thus the β domains and their TKs can move closer together and transphosphorylate, independent of the presence of insulin. A more limited deletion which removes part of L2 and most of the CD region activates IR and blunts the action of insulin¹⁸. Such a deletion removes the physical support for the CR cam region of the partner monomer, thus partly collapsing the cam to permit rapprochement of the TK regions. At the same time the geometry of the insulin binding site in the L2 and CR region would be affected, as well as the insulin-induced change in the relative configuration of the entire L1-CR-L2 regions.

Please replace the paragraph beginning at page 58, line 12 as follows:

More subtle alterations of IR are the mutations Phe383Val and Asp919Glu, both of which impair TK action^{5,20,21}. Phe383 is midway in the L2 domain¹⁰, which in the model is straddled by the Fn0 linkage to the α - α Cys524 disulphide bond and by the CR cam region of the partner monomer that contacts the Fn2/TM region. The Asp919Glu mutation is at the C-terminal edge of

the Fn2 domain of the β subunit (SEQ ID NO:17), which in the model contacts the cam. Size modifications in either of these complementary extracellular contact sites may prevent proper mating of the intracellular TK domains.